

Electronic Supplementary Information for

Conversion of a Non-Selective Adenosine Receptor Antagonist into A₃-Selective High Affinity Fluorescent Probes Using Peptide-Based Linkers

*Andrea J Vernall,^{a, b} Leigh A Stoddart,^{c, b} Stephen J Briddon,^c Hui Wen Ng,^d Charles A Laughton,^a
Stephen W Doughty,^d Stephen J Hill,^{c*} Barrie Kellam^{a*}*

^aSchool of Pharmacy, Centre for Biomolecular Sciences, University of Nottingham, University Park, Nottingham NG7 2RD, UK. ^c School of Pharmacy, University of Nottingham Malaysia Campus, Jalan Broga, 43500 Semenyih, Selangor Darul Ehsan, Malaysia. ^dInstitute of Cell Signalling, School of Biomedical Science, Queen's Medical Centre, University of Nottingham, Nottingham NG1 1GF, UK. * E-mail: barrie.kellam@nottingham.ac.uk, Tel: +44-115-9513026; E-mail: stephen.hill@nottingham.ac.uk, Tel: +44-115-8230082.

^bThese authors contributed equally to this work.

Table of Contents

Abbreviations	S3
Chemistry: General Material and Methods	S3
Chemistry: Synthesis and characterisation of 4 - 28	S5
Pharmacology: General Methods	S19
Supplementary Fig S1: Pharmacological analysis of 27 and 28	S22
Supplementary Table S2: Comparison of assay formats	S23
Stability of Fmoc-XAC compounds under assay conditions	S23
Supplementary Fig S2: Fmoc-compound stability under assay conditions	S24
Fluorescent Confocal Microscopy Imaging Studies	S25
Molecular Modelling	S26
Supplementary Fig S3: Ramachandran plot of hA ₁ AR model	S27
Supplementary Fig S4: Ramachandran plot of hA ₃ AR model	S28
Supplementary Fig S5 and Table S3: Predicted pK _i versus experimental pK _i for the A ₁ AR model	S28-S29
Supplementary Fig S6 and Table S4: Predicted pK _i versus experimental pK _i for the A ₁ AR model	S29-S30
Supplementary Fig S7: Molecular Modelling Visualisation	S30
References	S33-S40

Abbreviations

CA200645, (*E*)-3-(4-((1-(4-(2,6-dioxo-1,3-dipropyl-2,3,6,7-tetrahydro-1*H*-purin-8-yl)phenoxy)-2,7,11,17,24-pentaoxo-3,6,10,16,23-pentaazapentacosan-25-yl)oxy)styryl)-5,5-difluoro-7-(thiophen-2-yl)-5*H*-dipyrrolo[1,2-*c*:2',1'-*f*][1,3,2]diazaborinin-4-ium-5-uide; Ahx, 6-amino hexanoic acid; BODIPY 630/650-X, 6-(((4,4-difluoro-5-(2-thienyl)-4-bora-3*a*,4*a*-diazas-indacene-3-yl)styryloxy)acetyl)amino hexanoic acid; BODIPY-FL, 4,4-difluoro-5,7-dimethyl-4-bora-3*a*,4*a*-diazas-indacene-3-propionic acid; cAMP, cyclic adenosine monophosphate; CHO, chinese hamster ovary; CRE-SPAP, cAMP response element-secreted placental alkaline phosphatase; DPCPX, 8-cyclopentyl-1,3-dipropylxanthine; Fmoc; fluorenylmethyloxycarbonyl; FSK, forskolin; GPCR, G protein-coupled receptor; HATU, O-(7-Azabenzotriazol-1-yl)-*N,N,N',N'*-tetramethyluronium hexafluorophosphate; MD, molecular dynamics; NECA, adenosine-5-*N*-ethylcarboxamide; MRS1220, *N*-[9-chloro-2-(2-furanyl)[1,2,4]-triazolo[1,5-*c*]quinazolin-5-yl]benzene acetamide; POPC, palmitoyl-oleoyl-phosphatidylcholine; PLC, preparative layer chromatography; RP-HPLC, reversed-phase high pressure liquid chromatography; SE; succinimidyl ester; TM, transmembrane; XAC, xanthine amine congener.

Chemistry: General Materials and Methods.

Chemicals and solvents of an analytical grade were purchased from commercial suppliers and used without further purification. BODIPY-630/650-X-SE and BODIPY-FL-X-SE were purchased from Molecular Probes® (Invitrogen, UK). Unless otherwise stated, reactions were carried out at ambient temperature. Reactions were monitored by thin layer chromatography on commercially available pre-coated aluminium-backed plates (Merck Kieselgel 60 F254). Visualisation was by examination under UV light (254 and 366 nm), or staining with KMnO₄ dip. Flash chromatography was performed using Merck Kieselgel 60, 230-400 mesh (Merck KgaA, Darmstadt, Germany) on a Biotage Flashmaster II system. Silica plate chromatography was performed using Analtech Uniplate preparative layer chromatography plates with silica gel GF and UV254 (20×20 cm, 1000 microns).

¹H NMR spectra were recorded on a Bruker AV(II) 500 at 503.13 MHz at 25°C. ¹³C NMR spectra were recorded on a Bruker AV(II) 500 with a dual (CH) cryoprobe at 125.8 MHz at 25°C. Solvent used for NMR analysis (reference peaks listed) was DMSO-*d*₆ ((CHD₂)₂SO at δ_H 2.50 ppm, (CD₃)₂SO at 39.52 ppm). Chemical shifts (δ) are recorded in parts per million (ppm). Coupling constants (*J*) are recorded in Hz (rounded to one decimal point) and the significant multiplicities described by singlet (s), doublet (d), triplet (t), quadruplet (q), broad (br), and multiplet (m). Spectra were assigned using appropriate COSY, DEPT, HSQC and HMBC sequences. Copies of key NMR S3

spectra are shown at the end of the Supplementary Information (pages S33 - S40). High resolution mass spectra (HRMS) – time of flight, electrospray (TOF ES +/-) were recorded on a Waters 2795 separation module/micromass LCT platform.

RP-HPLC was performed using a Waters 2767 sample manager, Waters 2525 binary gradient module, and visualised at 254 nm and 366 nm with a Waters 2487 dual wavelength absorbance detector. Spectra were analysed using MassLynx. Preparative RP-HPLC was performed using a Phenomenex Luna C8(2) 11A Axia F column (150 mm × 30 mm × 10 μm) at a flow rate of 20 mL/min. Semi-preparative RP-HPLC was performed using a YMC-Pack C8 column (150 mm × 10 mm × 5 μm) at a flow rate of 3 mL/min. Analytical RP-HPLC was performed using a YMC-Pack C8 column (150 mm × 4.6 mm × 5 μm) at a flow rate of 1 mL/min. The retention time (R_t) of the final product for biological testing is reported using an analytical RP-HPLC method of 0 - 2 min 10% solvent B in solvent A, 2 – 20 min gradient of 10% to 80% solvent B in solvent A, 20 – 21 min 80% to 90% solvent B in solvent A, 21 – 23 min held at 90% B in solvent A, 23 – 24 min 90% to 10% solvent B in solvent A, 24 – 29 min held at 10% solvent B in solvent A (solvent A = 0.05% TFA in H₂O, solvent B = 0.05% TFA in 9:1 v:v CH₃CN:H₂O). Purities of all compounds tested in biological systems were determined by analytical RP-HPLC as being ≥95%. Copies of HPLC chromatograms are shown at the end of the Supplementary Information (pages S33-S40).

Chemistry: Synthesis and characterisation of compounds 4 - 28

Please note: NMR spectra of key compounds, and HRMS chromatograms for all biologically tested compounds are provided at the end of this Supplementary Information (pages S33 – S40).

General Procedure A: Peptide bond formation.

To a solution of the amine (1 equiv) in DMF was added a solution of the carboxylic acid (2 equiv), HATU (2 equiv) and DIPEA (4 equiv) in DMF. The solution was stirred for 4 h at rt, the solvent removed under reduced pressure, and the residue purified by flash silica column chromatography, preparative layer chromatography (PLC, using a silica plate), preparative RP-HPLC, or by precipitating in ethyl acetate.

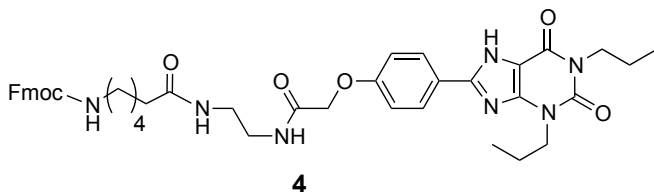
General Procedure B: Fmoc deprotection.

To the *N*- α -Fmoc-protected compound was added diethylamine:dichloromethane (1:1 v/v, 1–2 mL) and the mixture stirred for 2 h at rt. The solvent was then removed under reduced pressure and the residue washed with petroleum spirit, dried under high vacuum, and used without further purification.

General Procedure C: *tert*-Butyl ether cleavage.

To the compound containing a *tert*-butyl protected phenol, and/or *tert*-butyl protected alcohol, and/or trityl protected carboxamide was added trifluoroacetic acid:dichloromethane (1:1 v/v, 1–2 mL) and the mixture stirred for 1 h at rt. The solvent was then removed under reduced pressure and the residue washed with petroleum spirit, dried under high vacuum, and purified by preparative layer chromatography or by semi-preparative RP-HPLC.

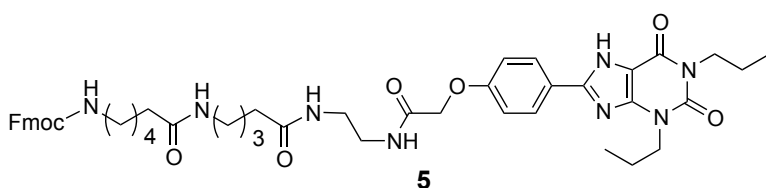
9*H*-Fluoren-9-ylmethyl *N*-{5-[(2-{2-[4-(2,6-dioxo-1,3-dipropyl-2,3,6,9-tetrahydro-1*H*-purin-8-yl)phenoxy]acetamido}ethyl)carbamoyl]pentyl}carbamate 4.



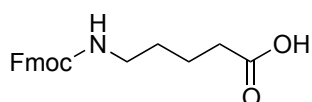
3 (12 μ mol) was treated with *N*-6-(9*H*-fluoren-9-ylmethoxycarbonyl)aminohexanoic acid (24 μ mol), HATU (24 μ mol) and DIPEA (48 μ mol) according to General Procedure A. The residue was purified by PLC (12% MeOH/DCM) to give **4** (8.8 mg, 10 μ mol, 83% from **3**) as a white solid. ^1H NMR (DMSO- d_6) δ 0.83 – 0.91 (m, 6H, CH₃), 1.19 (m, 2H, CH₂), 1.36 (m, 2H, CH₂), 1.47 (m, 2H, CH₂), 1.57 (m, 2H, CH₂), 1.73 (m, 2H, CH₂), 2.03 (m, 2H, CH₂), 2.93 (m, 2H, CH₂), 3.14 – 3.19 (m, 4H, CH₂), 3.86 (t, J = 7.5 Hz, 2H, CH₂), 4.00 (t, J = 7.2 Hz, 2H, CH₂), 4.19 (t, J = 7.0 Hz, 1H, S5

CH), 4.27 (d, $J = 6.8$ Hz, 2H, CH₂), 4.54 (s, 2H, CH₂), 7.09 (d, $J = 9.1$ Hz, 2H, ArH), 7.26 (t, $J = 5.7$ Hz, 1H, NH), 7.31 (m, 2H, ArH), 7.40 (m, 2H, ArH), 7.67 (d, $J = 7.7$ Hz, 2H, ArH), 7.86 – 7.88 (m, 3H, ArH, NH), 8.08 (d, $J = 9.0$ Hz, 2H, ArH), 8.20 (t, $J = 5.5$ Hz, 1H, NH), 13.65 (s, 1H, NH). ¹³C NMR (DMSO-*d*₆) δ 11.06, 11.20, 20.88, 24.94, 25.93, 29.18, 35.36, 38.06, 38.51, 40.79, 42.10, 44.37, 46.75, 65.13, 66.89, 107.37, 115.15, 120.12, 121.90, 125.14, 127.03, 127.59, 128.09, 140.73, 143.94, 148.37, 149.97, 150.65, 153.96, 156.05, 159.19, 167.50, 172.42. HRMS calculated for C₄₂H₅₀N₇O₇ 764.3772(M+H)⁺, found 764.3727. Analytical RP-HPLC $R_t = 20.7$ min.

9H-Fluoren-9-ylmethyl N-(5-((4-((2-(2-[4-(2,6-dioxo-1,3-dipropyl-2,3,6,9-tetrahydro-1H-purin-8-yl)phenoxy]acetamido)ethyl)carbamoyl]butyl)carbamoyl}pentyl)carbamate 5.



5-Aminopentanoic acid (1.7 mmol) was dissolved in water (6 mL) and sodium bicarbonate (5 mmol) was added. To this was added dioxane (6 mL) and Fmoc-succinimidyl ester (1.7 mmol), and the reaction stirred at rt overnight. Water (6 mL) was added, and the solution acidified to pH = 3 using 1M aqueous HCl. The precipitate was filtered, washed with cold water, and dried to give 5-(9H-fluoren-9-ylmethoxycarbonyl)aminopentanoic acid (502 mg, 1.5 mmol, 87% from 5-aminopentanoic acid) as a white solid.



¹H NMR (DMSO-*d*₆) δ 1.38 – 1.50 (m, 4H, CH₂), 2.20 (t, $J = 7.2$ Hz, 2H, CH₂), 2.97 (m, 2H, CH₂), 4.20 (t, $J = 6.7$ Hz, 1H, CH), 4.29 (d, $J = 6.7$ Hz, 2H, CH₂), 7.27 – 7.35 (m, 3H, ArH, NH), 7.41 (t, $J = 7.2$ Hz, 2H, ArH), 7.68 (d, $J = 7.5$ Hz, 2H, ArH), 7.88 (d, $J = 7.3$ Hz, 2H, ArH), 12.01 (br s, 1H, CO₂H).

3 (6.5 μ mol) was treated with 5-(9H-fluoren-9-ylmethoxycarbonyl)aminopentanoic acid (13 μ mol), HATU (13 μ mol) and DIPEA (26 μ mol) according to General Procedure A. The solvent was evaporated and ethyl acetate was added, and the precipitate was collected, washed with ethyl acetate, to give (9H-fluoren-9-yl)methyl (5-((2-(2-(4-(2,6-dioxo-1,3-dipropyl-2,3,6,9-tetrahydro-1H-purin-8-yl)phenoxy]acetamido)ethyl)amino)-5-oxopentyl)carbamate (4 mg, 5.3 μ mol, 82% from **3**) as a white solid. HRMS calculated for C₄₁H₄₈N₇O₇ 750.3610 (M+H)⁺, found 750.3638.

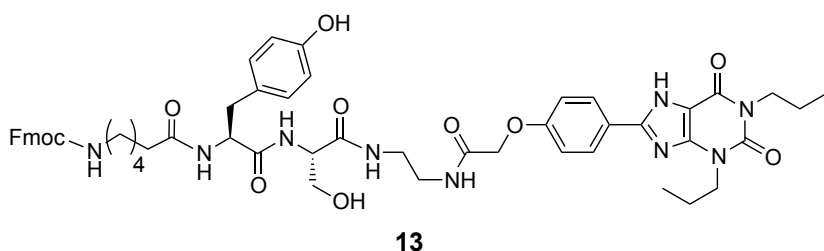
(9*H*-Fluoren-9-yl)methyl (5-((2-(2-(4-(2,6-dioxo-1,3-dipropyl-2,3,6,9-tetrahydro-1*H*-purin-8-yl)phenoxy)acetamido)ethyl)amino)-5-oxopentyl)carbamate (5.3 μmol) was treated with diethylamine in dichloromethane according to General Procedure B to give 5-amino-*N*-[(2-{2-[4-(2,6-dioxo-1,3-dipropyl-2,3,6,9-tetrahydro-1*H*-purin-8-yl)phenoxy]acetamido}ethyl)carbamoyl]pentanamide (assume quantitative). HRMS calculated for C₂₆H₃₈N₇O₅ 528.2929 (M+H)⁺; found 528.2926.

5-Amino-*N*-[(2-{2-[4-(2,6-dioxo-1,3-dipropyl-2,3,6,9-tetrahydro-1*H*-purin-8-yl)phenoxy]acetamido}-ethyl)carbamoyl]pentanamide (5.3 μmol) was treated with *N*-Fmoc-6-aminohexanoic acid (11 μmol), HATU (11 μmol) and DIPEA (22 μmol) according to General Procedure A. The residue was purified by PLC (12% MeOH/DCM) and then by semi-preparative RP-HPLC to afford **5** (2 mg, 2.3 μmol, 44% from (9*H*-fluoren-9-yl)methyl (5-((2-(2-(4-(2,6-dioxo-1,3-dipropyl-2,3,6,9-tetrahydro-1*H*-purin-8-yl)phenoxy)acetamido)ethyl)amino)-5-oxopentyl)carbamate) as a white solid. HRMS calculated for C₄₇H₅₉N₈O₈ 863.4450 (M+H)⁺; found 863.4414. Analytical RP-HPLC *R*_t = 19.6 min.

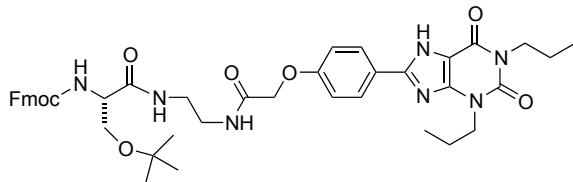
Synthesis of Fmoc-dipeptide-XAC library, compounds 6 - 14

Compounds **6-14** (Scheme 1 in main paper) were synthesised in an analogous manner using solution-phase peptide coupling methods. The synthetic procedures and compound characterisation of the intermediates for the synthesis of one representative library member from Scheme 1 (compound **13**) are specified below. Details of synthetic intermediates, methods, and yields for the other library compounds (**6 – 12, 14**) are provided in Supplementary Table 1. Copies of the HPLC chromatograms for biologically tested compounds are provided at the end of the Supplemental Information (pages S33 - S40).

9*H*-Fluoren-9-ylmethyl *N*-((5-((1*S*)-1-((1*S*)-1-((2-{2-[4-(2,6-dioxo-1,3-dipropyl-2,3,6,9-tetrahydro-1*H*-purin-8-yl)phenoxy]acetamido}ethyl)carbamoyl]-2-hydroxyethyl)carbamoyl]-2-(4-hydroxyphenyl)ethyl)carbamoyl]pentyl)carbamate **13**.

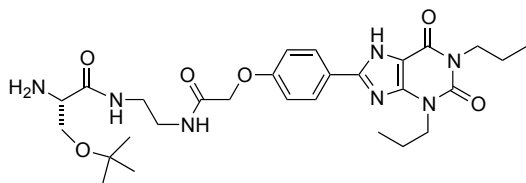


3 (100 mg, 0.23 mmol) was treated with Fmoc-Ser(tBu)-OH (0.46 mmol), HATU (0.46 mmol) and DIPEA (0.92 mmol) according to General Procedure A. The residue was purified by flash silica column chromatography (0-8% MeOH/DCM) to give 9*H*-fluoren-9-ylmethyl *N*-[(1*S*)-2-(*tert*-butoxy)-1-[(2-{2-[4-(2,6-dioxo-1,3-dipropyl-2,3,6,9-tetrahydro-1*H*-purin-8-yl)phenoxy]acetamido}ethyl)carbamoyl]-ethyl]carbamate (133 mg, 0.17 mmol, 73% from **3**) as a white solid.



^1H NMR (DMSO- d_6) δ 0.86 – 0.91 (m, 6H, CH₃), 1.09 (s, 9H, C(CH₃)₃), 1.58 (m, 2H, CH₂), 1.73 (m, 2H, CH₂), 3.15 – 3.22 (m, 4H, CH₂), 3.43 (m, 1H, CHH), 3.49 (m, 1H, CHH), 3.86 (t, J = 7.0 Hz, 2H, CH₂), 4.00 (t, J = 7.1 Hz, 2H CH₂), 4.05 (m, 1H, CH), 4.22 (m, 2H, CH₂), 4.28 (m, 1H, CH), 4.54 (s, 2H, CH₂), 7.09 (d, J = 8.7 Hz, 2H, ArH), 7.31 (t, J = 7.6 Hz, 2H, ArH), 7.36 – 7.42 (m, 3H, ArH, NH), 7.72 (t, J = 7.7 Hz, 2H, ArH), 7.88 (d, J = 7.8 Hz, 2H, ArH), 8.05 – 8.08 (m, 3H, ArH, NH), 8.18 (br m, 1H, NH), 13.65 (s, 1H, NH). ^{13}C NMR (DMSO- d_6) δ 11.06, 11.20, 20.88, 27.25, 38.22, 38.28, 42.10, 44.37, 46.61, 55.57, 61.84, 65.74, 66.91, 72.78, 107.35, 115.18, 120.11, 121.90, 125.35, 127.04, 127.64, 129.00, 140.70, 143.78, 148.37, 149.96, 150.65, 153.96, 155.88, 159.18, 167.51, 170.25. HRMS calculated for C₄₃H₅₂N₇O₈ 794.3877 (M+H)⁺; found 794.3870.

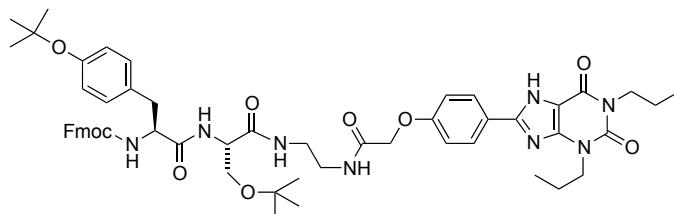
9*H*-Fluoren-9-ylmethyl *N*-[(1*S*)-2-(*tert*-butoxy)-1-[(2-{2-[4-(2,6-dioxo-1,3-dipropyl-2,3,6,9-tetrahydro-1*H*-purin-8-yl)phenoxy]acetamido}ethyl)carbamoyl]-ethyl]carbamate (0.10 mmol) was treated with diethylamine in dichloromethane according to General Procedure B to give (2*S*)-2-amino-3-(*tert*-butoxy)-*N*-(2-{2-[4-(2,6-dioxo-1,3-dipropyl-2,3,6,7-tetrahydro-1*H*-purin-8-yl)phenoxy]acetamido}ethyl)propanamide (assume quantitative).



HRMS calculated for C₂₈H₄₂N₇O₆ 572.3197 (M+H)⁺; found 572.3206.

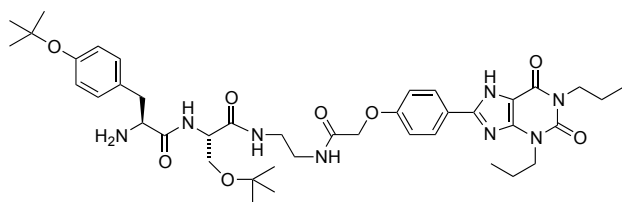
(2*S*)-2-Amino-3-(*tert*-butoxy)-*N*-(2-{2-[4-(2,6-dioxo-1,3-dipropyl-2,3,6,7-tetrahydro-1*H*-purin-8-yl)phenoxy]acetamido}ethyl)propanamide (0.10 mmol) was treated with Fmoc-Tyr(tBu)-OH (0.20 mmol), HATU (0.20 mmol) and DIPEA (0.40 mmol) according to General Procedure A. The residue was purified by flash silica column chromatography (0-8% MeOH/DCM) to give 9*H*-S8

fluoren-9-ylmethyl *N*-[(1*S*)-1-[(1*S*)-2-(*tert*-butoxy)-1-[(2-{2-[4-(2,6-dioxo-1,3-dipropyl-2,3,6,7-tetrahydro-1*H*-purin-8-yl)phenoxy]acetamido}ethyl)carbamoyl]ethyl]carbamoyl]-2-[4-(*tert*-butoxy)phenyl]ethyl]carbamate **18** (67 mg, 0.07 mmol, 66% from 9*H*-fluoren-9-ylmethyl *N*-[(1*S*)-2-(*tert*-butoxy)-1-[(2-{2-[4-(2,6-dioxo-1,3-dipropyl-2,3,6,9-tetrahydro-1*H*-purin-8-yl)phenoxy]acetamido}ethyl)carbamoyl]-ethyl]carbamate) as a white solid.



^1H NMR (DMSO- d_6) δ 0.86 – 0.91 (m, 6H, CH₃), 1.08 (s, 9H, C(CH₃)₃), 1.15 (s, 9H, C(CH₃)₃), 1.58 (m, 2H, CH₂), 1.73 (m, 2H, CH₂), 2.71 (m, 1H, tyr CHH), 2.98 (m, 1H, tyr CHH), 3.13 – 3.23 (m, 4H, CH₂), 3.45 (m, 2H, ser CH₂), 3.61 (m, 2H, CH₂), 3.86 (t, J = 7.3 Hz, 2H, CH₂), 4.00 (t, J = 7.3 Hz, 2H, CH₂), 4.08 – 4.16 (m, 3H, CH₂, CH), 4.28 – 4.32 (m, 2H, CH), 4.54 (s, 2H, CH₂), 6.77 (d, J = 8.3 Hz, 2H, ArH), 7.10 (d, J = 9.1 Hz, 2H, ArH), 7.18 (d, J = 8.3 Hz, 2H, ArH), 7.29 (m, 2H, ArH), 7.39 (t, J = 7.6 Hz, 2H, ArH), 7.63 (m, 2H, ArH), 7.67 (d, J = 8.9 Hz, 1H, NH), 7.86 (d, J = 7.9 Hz, 2H, ArH), 7.97 (d, J = 8.3 Hz, 1H, NH), 8.04 (br m, 1H, NH), 8.08 (d, J = 9.1 Hz, 2H, ArH), 8.19 (br m, 1H, NH), 13.65 (s, 1H, NH). ^{13}C NMR (DMSO- d_6) δ 11.07, 11.21, 20.88, 27.18, 28.45, 36.69, 38.28, 41.84, 42.11, 44.37, 46.52, 53.54, 53.74, 56.06, 61.83, 65.72, 66.90, 72.80, 77.48, 107.35, 115.18, 120.67, 121.90, 123.23, 125.33, 127.05, 127.62, 128.11, 128.82, 129.77, 140.68, 143.72, 148.37, 149.97, 150.98, 153.31, 153.96, 155.85, 159.17, 167.52, 169.91, 171.48. HRMS calculated for C₅₆H₆₉N₈O₁₀ 1013.5131 (M+H)⁺; 1013.5141.

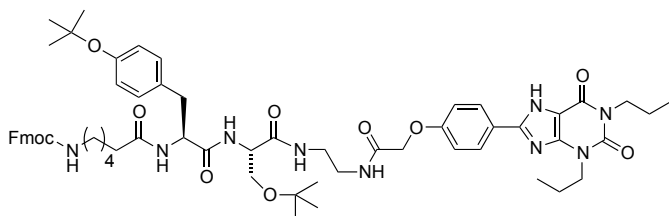
Compound **18** (30 mg, 0.03 mmol) was treated with diethylamine in dichloromethane according to General Procedure B to give (2*S*)-2-[(2*S*)-2-amino-3-[4-(*tert*-butoxy)phenyl]propanamido]-3-(*tert*-butoxy)-*N*-(2-{2-[4-(2,6-dioxo-1,3-dipropyl-2,3,6,7-tetrahydro-1*H*-purin-8-yl)phenoxy]acetamido}ethyl)propanamide (assume assume quantitative).



HRMS calculated for C₄₁H₅₉N₈O₈ 791.4456 (M+H)⁺; found 791.4648.

(2*S*)-2-[(2*S*)-2-amino-3-[4-(*tert*-butoxy)phenyl]propanamido]-3-(*tert*-butoxy)-*N*-(2-{2-[4-(2,6-dioxo-1,3-dipropyl-2,3,6,7-tetrahydro-1*H*-purin-8-yl)phenoxy]acetamido}ethyl)propanamide (0.03 mmol) was reacted with *N*-Fmoc-6-aminohexanoic acid (0.06 mmol), HATU (0.06 mmol) and S9

DIPEA (0.12 mmol) according to General Procedure A. The residue was purified using PLC (15% MeOH/DCM) to afford 9*H*-fluoren-9-ylmethyl *N*-(5-{[(1*S*)-1-{[(1*S*)-2-(tert-butoxy)-1-[(2-{2-[4-(2,6-dioxo-1,3-dipropyl-2,3,6,9-tetrahydro-1*H*-purin-8-yl)phenoxy]acetamido}ethyl)carbamoyl]ethyl]carbamoyl}-2-[4-(tert-butoxy)phenyl]ethyl]carbamoyl}pentyl)carbamate (24 mg, 0.02 mmol, 71% from **18**) as an off white solid.



^1H NMR (DMSO- d_6) δ 0.86 – 0.91 (m, 6H, CH₃), 1.07 – 1.11 (m, 11H, C(CH₃)₃, CH₂), 1.20 (s, 9H, C(CH₃)₃), 1.29 – 1.35 (m, 4H, CH₂), 1.58 (m, 2H, CH₂), 1.73 (m, 2H, CH₂), 2.00 (m, 2H, CH₂), 2.67 (m, 1H, tyr CHH), 2.90 (m, 2H, CH₂), 2.97 (m, 1H, tyr CHH), 3.16 – 3.24 (m, 4H, CH₂), 3.45 (m, 2H, ser CH₂), 3.86 (t, J = 7.4 Hz, 2H, CH₂), 4.01 (t, J = 7.3 Hz, 2H, CH₂), 4.19 (t, J = 6.9 Hz, 1H, CH), 4.23 – 4.28 (m, 3H, CH₂, CH), 4.53 – 4.55 (m, 3H, CH₂, CH), 6.80 (d, J = 8.5 Hz, 2H, ArH), 7.09 – 7.13 (m, 4H, ArH), 7.23 (t, J = 5.7 Hz, 1H, NH), 7.31 (m, 2H, ArH), 7.40 (t, J = 7.4 Hz, 2H, ArH), 7.67 (d, J = 7.5 Hz, 2H, ArH), 7.85 (m, 1H, NH), 7.88 (m, 2H, ArH), 7.97 (br m, 1H, NH), 8.05 – 8.08 (m, 3H, ArH, NH), 8.19 (br m, 1H, NH), 13.65 (s, 1H, NH). ^{13}C NMR (DMSO- d_6) δ 11.07, 11.20, 20.88, 21.04, 24.11, 25.00, 25.79, 27.18, 28.49, 29.09, 35.17, 36.43, 38.29, 40.74, 42.10, 44.37, 46.76, 53.53, 53.71, 61.74, 65.13, 66.90, 72.78, 77.51, 107.35, 115.17, 120.13, 121.90, 123.28, 125.14, 127.03, 127.59, 128.11, 129.64, 132.73, 140.74, 143.94, 148.37, 149.96, 150.66, 153.25, 153.96, 156.03, 159.17, 167.51, 169.88, 171.44, 172.18. HRMS calculated for C₆₂H₈₀N₉O₁₁ 1126.5977 (M+H)⁺; found 1126.6029.

9*H*-Fluoren-9-ylmethyl *N*-(5-{[(1*S*)-1-{[(1*S*)-2-(tert-butoxy)-1-[(2-{2-[4-(2,6-dioxo-1,3-dipropyl-2,3,6,9-tetrahydro-1*H*-purin-8-yl)phenoxy]acetamido}ethyl)carbamoyl]ethyl]carbamoyl}-2-[4-(tert-butoxy)phenyl]ethyl]carbamoyl}pentyl)carbamate (12 mg, 0.01 mmol) was treated with trifluoroacetic acid in dichloromethane according to General Procedure C. The residue was purified using PLC (12% MeOH/DCM) to afford **13** (9 mg, 0.009 mmol, 89% from 9*H*-fluoren-9-ylmethyl *N*-(5-{[(1*S*)-1-{[(1*S*)-2-(tert-butoxy)-1-[(2-{2-[4-(2,6-dioxo-1,3-dipropyl-2,3,6,9-tetrahydro-1*H*-purin-8-yl)phenoxy]acetamido}ethyl)carbamoyl]ethyl]carbamoyl}-2-[4-(tert-butoxy)phenyl]ethyl]carbamoyl}pentyl)carbamate) as an off white solid. ^1H NMR (DMSO- d_6) δ 0.86 – 0.91 (m, 6H, CH₃), 1.10 (m, 2H, CH₂), 1.31 – 1.38 (m, 4H, CH₂), 1.58 (m, 2H, CH₂CH₃), 1.74 (m, 2H, CH₂CH₃), 2.02 (t, J = 7.5 Hz, 2H, COCH₂CH₂), 2.62 (m, 1H, tyr CHH), 2.90 – 2.94 (m, 3H, tyr CHH, CONHCH₂), 3.16 – 3.24 (m, 4H, NHCH₂CH₂NH), 3.57 (m, 2H, ser CH₂), 3.86 (t,

$J = 7.4$ Hz, 2H, NCH₂), 4.01 (t, $J = 7.1$ Hz, 2H, NCH₂), 4.18 – 4.21 (m, 2H, tyr CH, Fmoc CH), 4.28 (d, $J = 7.1$ Hz, 2H, Fmoc CH₂), 4.46 (m, 1H, ser CH), 4.54 (s, 2H, COCH₂O), 4.92 (t, $J = 5.6$ Hz, 1H, ser OH), 6.62 (d, $J = 8.5$ Hz, 2H, tyr ArH), 7.02 (d, $J = 8.5$ Hz, 2H, tyr ArH), 7.09 (d, $J = 9.0$ Hz, 2H, XAC ArH), 7.24 (t, $J = 5.7$ Hz, 1H, CONHCH₂), 7.32 (m, 2H, Fmoc ArH), 7.40 (t, $J = 7.5$ Hz, 2H, Fmoc ArH), 7.67 (d, $J = 7.6$ Hz, 2H, Fmoc ArH), 7.85 (m, 1H, NHCH₂CH₂NH), 7.88 (d, $J = 7.6$ Hz, 2H, Fmoc ArH), 7.92 (d, $J = 7.6$ Hz, 1H, ser NH), 7.98 (d, $J = 8.0$ Hz, 1H, tyr NH), 8.08 (d, $J = 9.0$ Hz, 2H, XAC ArH), 8.18 (br m, 1H, NHCH₂CH₂NH), 9.14 (s, 1H, tyr OH), 13.65 (s, 1H, XAC NH). ¹³C NMR (DMSO-*d*₆) δ 11.08, 11.21, 20.89, 20.90, 24.12, 24.95, 25.80, 29.19, 35.17, 36.55, 38.13, 38.38, 42.11, 44.38, 46.77, 54.24, 55.25, 61.60, 65.14, 66.89, 107.36, 114.76, 115.18, 120.13, 121.89, 125.16, 127.05, 127.60, 128.08, 128.12, 130.09, 140.74, 143.95, 148.38, 149.97, 150.66, 153.97, 155.69, 156.06, 159.18, 167.58, 170.11, 171.60, 172.25. HRMS calculated for C₅₄H₆₄N₉O₁₁ 1014.4725 (M+H)⁺; found 1014.4761. Analytical RP-HPLC $R_t = 19.2$ min.

Supplementary Table S1: Analytical data for compounds 6 -12, 14.

A representative example (compound **13**) from the Fmoc-dipeptide-XAC library synthesis (refer to main paper, Scheme 1) is given in detail in the proceeding section (pages S7 - S11). For compounds **6-12** and **14**, the reaction yields of the coupling reactions between **3** and the first sequential amino acid are given (e.g. for Fmoc-Ser(tBu)-XAC), and thereafter the yield of the final test compound (**6-12** and **14**) is reported as percentage recovery from this XAC-amino-acid-Fmoc building block. (e.g. the yield of Fmoc-Ahx-Ala-Ser-XAC (compound **10**) is reported as a yield from Fmoc-Ser(tBu)-XAC).

^a refers to General Procedures described in Supplementary Information. ^b ppt, precipitation in ethyl acetate then filter and wash; PLC (preparative layer chromatography), silica plate chromatography with 5 – 15 % MeOH/DCM; column, flash silica column chromatography eluting with 0 to 10% MeOH/DCM; HPLC (semi-preparative RP-HPLC) using methods outlined in General Materials and Methods section. ^c The synthesis of these compounds is reported in detail as intermediates during the synthesis of compound **13** (pages S7 - S11).

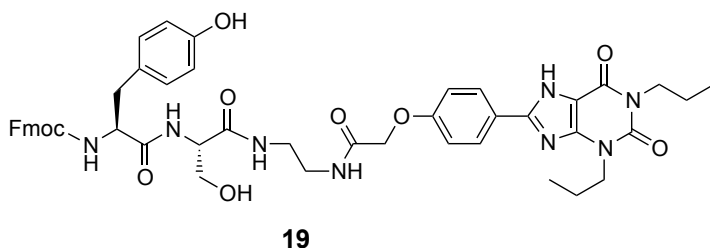
Compound Description	General Procedure ^a	Purification Method ^b	Mass Yield	Molecular Formula	HRMS Calc. (M+H) ⁺	HRMS Found	Analytical RP-HPLC R _t for test compounds
Fmoc-Ala-XAC	A	Ppt	65 mg, 97% from XAC 3	C ₃₉ H ₄₄ N ₇ O ₇	722.3302	722.3292	
Ala-XAC	B	-	-	C ₂₄ H ₃₄ N ₇ O ₅	500.2621	500.2641	
Fmoc-Ala-Ala-XAC	A	PLC	-	C ₄₂ H ₄₉ N ₈ O ₈	793.8867	793.8854	
Ala-Ala-XAC	B	-	-	C ₂₇ H ₃₉ N ₈ O ₆	571.2993	571.2997	
Fmoc-Ahx-Ala-Ala-XAC 6	A	HPLC	1.4 mg, 7% from Fmoc-Ala-XAC	C ₄₈ H ₆₀ N ₉ O ₉	906.4514	906.4551	19.5 min
Fmoc-Ser(tBu)-Ala-XAC 15	A	PLC	-	C ₄₆ H ₅₇ N ₈ O ₉	865.4249	865.4203	
Ser(tBu)-Ala-XAC	B	-	-	C ₃₁ H ₄₇ N ₈ O ₇	643.3568	643.3555	
Fmoc-Ahx-Ser(tBu)-Ala-XAC	A	Ppt	-	C ₅₂ H ₆₈ N ₉ O ₁₀	978.5089	978.507	
Fmoc-Ahx-Ser-Ala-XAC 7	C	PLC	4.0 mg, 20% from Fmoc-Ala-XAC	C ₄₈ H ₆₀ N ₉ O ₁₀	922.4463	922.4421	19.0 min
Fmoc-Tyr(tBu)-Ala-XAC 16	A	PLC	-	C ₅₂ H ₆₁ N ₈ O ₉	941.4562	941.4582	
Tyr(tBu)-Ala-XAC	B	-	-	C ₃₇ H ₅₁ N ₈ O ₇	719.3881	719.3882	
Fmoc-Ahx-Tyr(tBu)-Ala-XAC	A	PLC	-	C ₅₈ H ₇₂ N ₉ O ₁₀	1054.5402	1054.5419	
Fmoc-Ahx-Tyr-Ala-XAC 8	C	PLC	2.8 mg, 13% from Fmoc-Ala-XAC	C ₅₄ H ₆₄ N ₉ O ₁₀	998.4776	998.4724	20.0 min
Fmoc-Asn(Trt)-Ala-XAC	A	PLC	-	C ₆₂ H ₆₄ N ₉ O ₉	1078.4827	1078.4879	
Asn(Trt)-Ala-XAC	B	-	-	C ₄₇ H ₅₄ N ₉ O ₇	856.4146	856.4105	
Fmoc-Ahx-Asn(Trt)-Ala-XAC	A	PLC	-	C ₆₈ H ₇₅ N ₁₀ O ₁₀	1191.5668	1191.5679	
Fmoc-X-Asn-Ala-XAC 9	C	HPLC	1.3 mg, 6% from Fmoc-Ala-XAC	C ₄₉ H ₆₁ N ₁₀ O ₁₀	949.4572	949.451	18.6 min
Fmoc-Ser(tBu)-XAC	A	column	133 mg, 73% from XAC	C ₄₃ H ₅₂ N ₇ O ₈	794.3877	794.387	
Ser(tBu)-XAC	B	-	-	C ₂₈ H ₄₂ N ₇ O ₆	572.3197	572.3206	
Fmoc-Ala-Ser(tBu)-XAC	A	Ppt	-	C ₄₆ H ₅₇ N ₈ O ₉	865.4249	865.4259	
Ala-Ser(tBu)-XAC	B	-	-	C ₃₁ H ₄₇ N ₈ O ₇	643.3568	643.3562	
Fmoc-Ahx-Ala-Ser(tBu)-XAC	A	PLC	-	C ₅₂ H ₆₈ N ₉ O ₁₀	978.5089	978.5071	
Fmoc-Ahx-Ala-Ser-XAC 10	C	PLC	7.1 mg, 48% from Fmoc-Ser(tBu)-XAC	C ₄₈ H ₆₀ N ₉ O ₁₀	922.4463	922.4441	18.9 min
Fmoc-Tyr(tBu)-XAC	A	Ppt	17 mg, 85% from XAC	C ₄₉ H ₅₆ N ₇ O ₈	870.419	870.414	
Tyr(tBu)-XAC	B	-	-	C ₃₄ H ₄₆ N ₇ O ₆	648.351	648.3483	
Fmoc-Ala-Tyr(tBu)-XAC	A	Ppt	-	C ₅₂ H ₆₁ N ₈ O ₉	941.4562	941.4602	
Ala-Tyr(tBu)-XAC	B	-	-	C ₃₇ H ₅₁ N ₈ O ₇	719.3881	719.3882	
Fmoc-Ahx-Ala-Tyr(tBu)-XAC	A	PLC	-	C ₅₈ H ₇₂ N ₉ O ₁₀	1054.5402	1054.5392	
Fmoc-Ahx-Ala-Tyr-XAC 11	C	PLC	2.5 mg, 13% from Fmoc-Tyr(tBu)-XAC	C ₅₄ H ₆₄ N ₉ O ₁₀	998.4776	998.4712	19.9 min
Fmoc-Asn(Trt)-XAC	A	Ppt	19 mg, 80% from XAC	C ₅₉ H ₅₉ N ₈ O ₈	1007.4456	1007.4501	

Compound Description	General Procedure ^a	Purification Method ^b	Mass Yield	Molecular Formula	HRMS Calc. (M+H) ⁺	HRMS Found	Analytical RP-HPLC <i>R_t</i> for test compounds
Asn(trt)-XAC	B	-	-	C ₄₄ H ₄₉ N ₈ O ₆	785.3775	785.3724	
Fmoc-Ala-Asn(Trt)-XAC 17	A	Ppt	-	C ₆₂ H ₆₄ N ₉ O ₉	1078.4827	1078.4773	
Ala-Asn(Trt)-XAC	B	-	-	C ₄₇ H ₅₄ N ₉ O ₇	856.4146	856.4149	
Fmoc-Ahx-Ala-Asn(Trt)-XAC	A	PLC	-	C ₆₈ H ₇₅ N ₁₀ O ₁₀	1191.5668	1191.5668	
Fmoc-Ahx-Ala-Asn-XAC 12	C	PLC	4.8 mg, 25% from Fmoc-Asn(trt)-XAC	C ₄₉ H ₆₁ N ₁₀ O ₁₀	949.4572	949.4564	18.6 min
Fmoc-Tyr(tBu)-Ser(tBu)- XAC 18^c	A	column	67 mg, 66% from Fmoc-Ser(tBu)-XAC	C ₅₆ H ₆₉ N ₈ O ₁₀	1013.5137	1013.5141	
Tyr(tBu)-Ser(tBu)- XAC ^c	B	-	-	C ₄₁ H ₅₉ N ₈ O ₈	791.4456	791.4648	
Fmoc-Ahx-Tyr(tBu)-Ser(tBu)- XAC ^c	A	PLC	24 mg, 71% from Fmoc-Tyr(tBu)-Ser(tBu)-XAC	C ₆₂ H ₈₀ N ₉ O ₁₁	1126.5977	1126.6029	
Fmoc-Ahx-Tyr-Ser-XAC 13^c	C	PLC	9 mg, 89% from Fmoc-X-Tyr(tBu)-Ser(tBu)-XAC	C ₅₄ H ₆₄ N ₉ O ₁₁	1014.4725	1014.4761	19.2 min
Fmoc-Tyr(tBu)-Tyr(tBu)-XAC	A	PLC	-	C ₆₂ H ₇₃ N ₈ O ₁₀	1089.5444	1089.5487	
Tyr(tBu)-Tyr(tBu)-XAC	B	-	-	C ₄₇ H ₆₃ N ₈ O ₈	867.4763	867.4741	
Fmoc-Ahx-Tyr(tBu)-Tyr(tBu)-XAC	A	PLC	-	C ₆₈ H ₈₄ N ₉ O ₁₁	1202.6285	1202.63	
Fmoc-Ahx-Tyr-Tyr-XAC 14	C	HPLC	1.4 mg, 5% from Fmoc-Tyr(tBu)-XAC	C ₆₀ H ₆₈ N ₉ O ₁₁	1090.5033	1090.5028	20.4 min

Compounds 15 – 18.

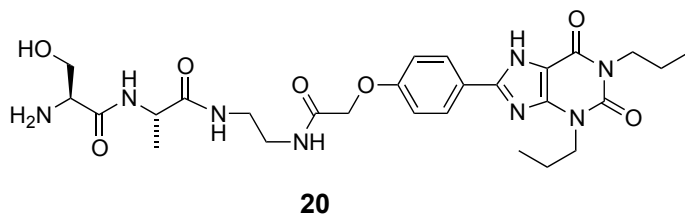
These compounds are intermediates in the synthesis of **7** (compound **15** is an intermediate), **8** (compound **16** is an intermediate), **12** (compound **17** is an intermediate), and **13** (compound **18** is an intermediate). The purification methods and HRMS parent ions are listed in Supplementary Table One.

(9H-Fluoren-9-yl)methyl ((S)-1-(((S)-1-((2-(2-(4-(2,6-dioxo-1,3-dipropyl-2,3,6,7-tetrahydro-1H-purin-8-yl)phenoxy)acetamido)ethyl)amino)-3-hydroxy-1-oxopropan-2-yl)amino)-3-(4-hydroxyphenyl)-1-oxopropan-2-yl)carbamate 19.



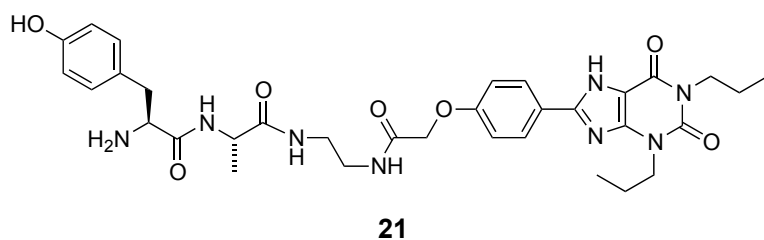
Fmoc-protected **18** (3 mg, 3 μ mol), an intermediate in the synthesis of **13**, was deprotected according to General Procedure C. The residue was purified by silica plate (12% MeOH/DCM) to give **19** (1.5 mg, 1.7 μ mol, 57% from **18**) as a white solid. HRMS calculated for $C_{48}H_{53}N_8O_{10}$ 901.3879 (M+H)⁺; found 901.3915. Analytical RP-HPLC R_t = 18.8 min.

(S)-2-Amino-N-(((S)-1-((2-(2-(4-(2,6-dioxo-1,3-dipropyl-2,3,6,7-tetrahydro-1H-purin-8-yl)phenoxy)acetamido)ethyl)amino)-1-oxopropan-2-yl)-3-hydroxypropanamide 20.



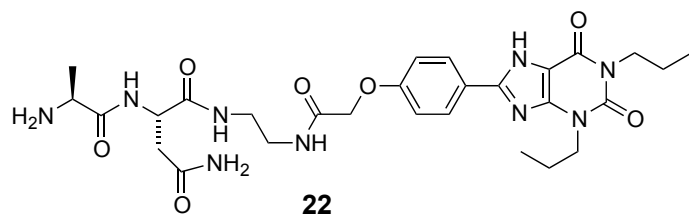
Fmoc-protected **15** (20 μ mol), an intermediate in the synthesis of **7** (refer to Supplementary Table One), was deprotected according to General Procedure B, to afford (S)-2-amino-3-(tert-butoxy)-N-(((S)-1-((2-(2-(4-(2,6-dioxo-1,3-dipropyl-2,3,6,7-tetrahydro-1H-purin-8-yl)phenoxy)acetamido)ethyl)amino)-1-oxopropan-2-yl)propanamide (HRMS calculated for $C_{31}H_{47}N_8O_7$ 643.3562 (M+H)⁺; found 643.3573). This was then side-chain deprotected by reaction according to General Procedure C to give side-chain deprotected **20**. The crude residue was used without further purification, and the yield assumed quantitative. HRMS calculated for $C_{27}H_{39}N_8O_7$ 587.2936 (M+H)⁺; found 587.2962.

(*S*)-2-Amino-*N*-((*S*)-1-((2-(2-(4-(2,6-dioxo-1,3-dipropyl-2,3,6,7-tetrahydro-1*H*-purin-8-yl)phenoxy)acetamido)ethyl)amino)-1-oxopropan-2-yl)-3-(4-hydroxyphenyl)propanamide **21.**



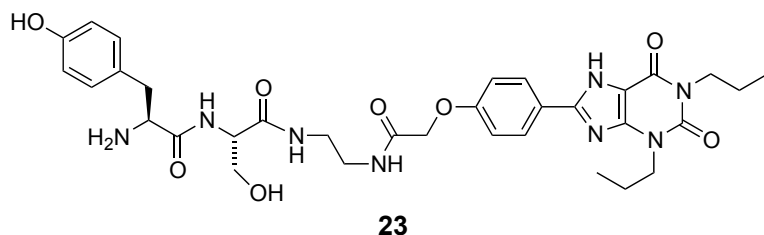
Fmoc-protected **16** (10 μ mol), an intermediate in the synthesis of **8** (refer to Supplementary Table One), was deprotected according to General Procedure B, to afford (*S*)-2-amino-3-(4-(tert-butoxy)phenyl)-*N*-((*S*)-1-((2-(2-(4-(2,6-dioxo-1,3-dipropyl-2,3,6,7-tetrahydro-1*H*-purin-8-yl)phenoxy)acetamido)ethyl)amino)-1-oxopropan-2-yl)propanamide (HRMS calculated for $C_{37}H_{51}N_8O_7$ 719.3875 ($M+H$)⁺; found 719.3855). This was then side-chain deprotected by reaction according to General Procedure C to give side-chain deprotected **21**. The crude residue was used without further purification, and the yield assumed quantitative. HRMS calculated for $C_{33}H_{43}N_8O_7$ 663.3249 ($M+H$)⁺; found 663.3263.

(*S*)-2-((*S*)-2-Aminopropanamido)-*N*¹-(2-(2-(4-(2,6-dioxo-1,3-dipropyl-2,3,6,7-tetrahydro-1*H*-purin-8-yl)phenoxy)acetamido)ethyl)succinamide **22.**



Fmoc-protected **17** (10 μ mol), an intermediate in the synthesis of **12** (refer to Supplementary Table One), was deprotected according to General Procedure B, to afford (*S*)-2-((*S*)-2-aminopropanamido)-*N*¹-(2-(2-(4-(2,6-dioxo-1,3-dipropyl-2,3,6,7-tetrahydro-1*H*-purin-8-yl)phenoxy)acetamido)ethyl)-*N*⁴-tritylsuccinamide (HRMS calculated for $C_{47}H_{54}N_9O_7$ 856.4146 ($M+H$)⁺; found 856.4149). This was then side-chain deprotected by reaction according to General Procedure C to give side-chain deprotected **22**. The crude residue was used without further purification, and the yield assumed quantitative. HRMS calculated for $C_{28}H_{40}N_9O_7$ 614.3045 ($M+H$)⁺; found 614.3065.

(*S*)-2-Amino-*N*-((*S*)-1-((2-(2-(4-(2,6-dioxo-1,3-dipropyl-2,3,6,9-tetrahydro-1*H*-purin-8-yl)phenoxy)acetamido)ethyl)amino)-3-hydroxy-1-oxopropan-2-yl)-3-(4-hydroxyphenyl)propanamide 23.

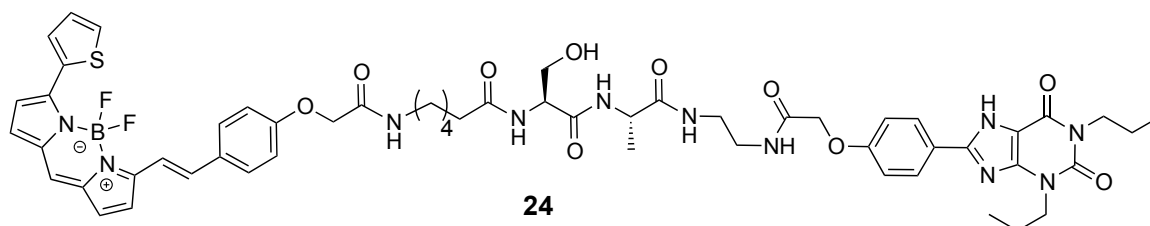


Fmoc-protected **18** (25 mg, 25 μ mol), an intermediate in the synthesis of **13**, was deprotected according to General Procedure B, to afford (*S*)-2-amino-*N*-((*S*)-3-(*tert*-butoxy)-1-((2-(2-(4-(2,6-dioxo-1,3-dipropyl-2,3,6,9-tetrahydro-1*H*-purin-8-yl)phenoxy)acetamido)ethyl)amino)-1-oxopropan-2-yl)-3-(4-(*tert*-butoxy)phenyl)propanamide (HRMS calculated for $C_{41}H_{59}N_8O_8$ 791.4456 ($M+H$)⁺; found 791.4648). The residue was then used in the next reaction without purification (assume quantitative yield). The residue (assuming 25 μ mol) was reacted according to General Procedure C to give **23**. The crude product was divided into five equal portions (assume 5 μ mol each), and one of these portions was purified by semi-preparative RP-HPLC (giving a white solid, 0.8 mg) for material suitable for biological testing. HRMS calculated for $C_{33}H_{43}N_8O_8$ 679.3204 ($M+H$)⁺; found 679.3169. Analytical RP-HPLC R_t = 13.7 min.

General Procedure D: Synthesis of 24 - 28.

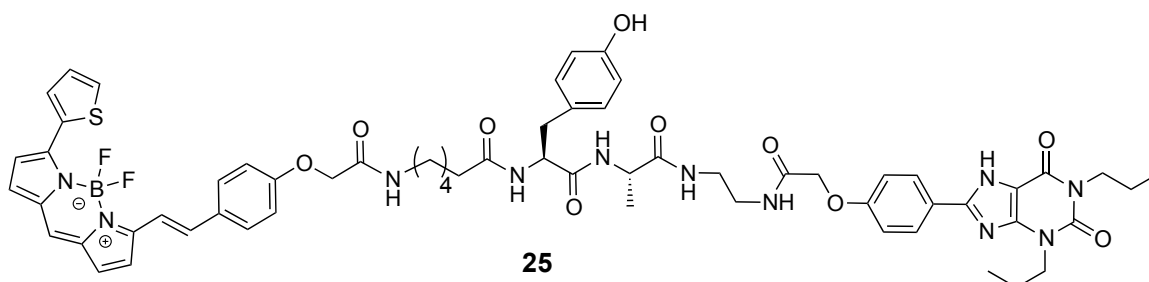
A solution of the amine (2-7 equiv), DIEPA (4 equiv) and the fluorophore-SE (1 equiv) was stirred in DMF (1 - 1.5 mL) with the exclusion of light for 12 h. The solvent was removed under reduced pressure, and the residue purified by silica plate and/or semi-preparative RP-HPLC.

***N*-[(1*S*)-1-[(1*S*)-1-[(2-{2-[4-(2,6-Dioxo-1,3-dipropyl-2,3,6,9-tetrahydro-1*H*-purin-8-yl)phenoxy]acetamido}ethyl)carbamoyl]ethyl]carbamoyl]-2-hydroxyethyl]-(*E*)-6-((4-(2-(4,4-difluoro-5-(2-thienyl)-4-bora-3a,4a-diaza-s-indacene-3-yl)vinyl)phenoxy)acetamido)hexanamide 24.**



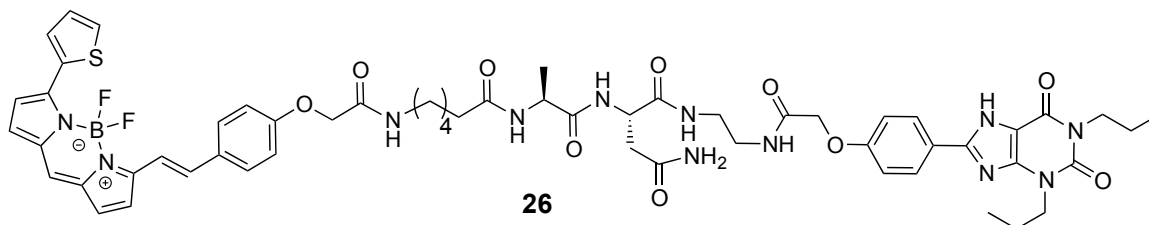
Compound **20** (10 μmol) was reacted with BODIPY 630/650-X-SE (2.4 μmol) according to General Procedure D. The residue was purified by preparative layer chromatography (15% MeOH/DCM) and then by semi-preparative RP-HPLC to give **24** (1.1 mg, 1 μmol , 41% from BODIPY 630/650-X-SE) as a blue solid. HRMS calculated for $\text{C}_{56}\text{H}_{65}\text{BF}_2\text{N}_{11}\text{O}_{10}\text{S}$ 1132.4692 ($\text{M}+\text{H}$)⁺; found 1132.4637. Analytical RP-HPLC R_t = 20.4 min.

N-[(1*S*)-1-[(1*S*)-1-[(2-{2-[4-(2,6-Dioxo-1,3-dipropyl-2,3,6,9-tetrahydro-1*H*-purin-8-yl)phenoxy]acetamido}ethyl)carbamoyl]ethyl]carbamoyl]-2-(4-hydroxyphenyl)ethyl]-(*E*)-6-((4-(2-(4,4-difluoro-5-(2-thienyl)-4-bora-3a,4a-diaza-*s*-indacene-3-yl)vinyl)phenoxy)acetamido)-hexanamide **25**.



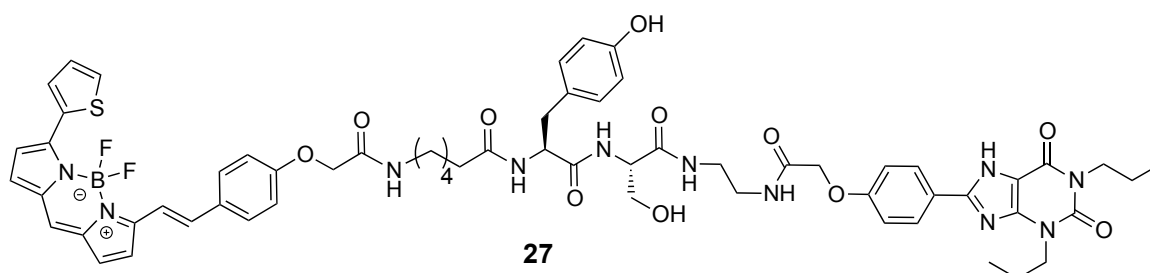
Compound **21** (10 μmol) was reacted with BODIPY 630/650-X-SE (1.5 μmol) according to General Procedure D. The residue was purified by preparative layer chromatography (15% MeOH/DCM) and then by semi-preparative RP-HPLC to give **25** (0.5 mg, 0.4 μmol , 28% from BODIPY 630/650-X-SE) as a blue solid. HRMS calculated for $\text{C}_{62}\text{H}_{69}\text{BF}_2\text{N}_{11}\text{O}_{10}\text{S}$ 1208.5005 ($\text{M}+\text{H}$)⁺; found 1208.5049. Analytical RP-HPLC R_t = 21.4 min.

N-[(1*S*)-1-[(1*S*)-1-[(2-{2-[4-(2,6-Dioxo-1,3-dipropyl-2,3,6,9-tetrahydro-1*H*-purin-8-yl)phenoxy]acetamido}ethyl)carbamoyl]-3-amino-3-oxopropyl]carbamoyl]ethyl]-(*E*)-6-((4-(2-(4,4-difluoro-5-(2-thienyl)-4-bora-3a,4a-diaza-*s*-indacene-3-yl)vinyl)phenoxy)acetamido)-hexanamide **26**.



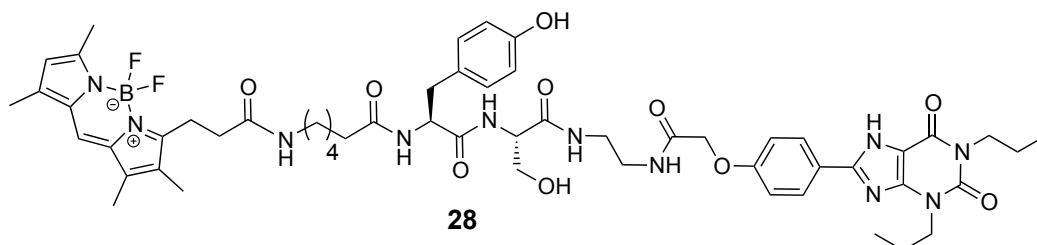
Compound **22** (10 μmol) was reacted with BODIPY 630/650-X-SE (1.5 μmol) according to General Procedure D. The residue was purified by preparative RP-HPLC to give **26** (0.9 mg, 0.77 μmol , 52% from BODIPY 630/650-X-SE) as a blue solid. HRMS calculated for $\text{C}_{57}\text{H}_{66}\text{BF}_2\text{N}_{12}\text{O}_{10}\text{S}$ 1159.4801 ($\text{M}+\text{H}$)⁺; found 1159.4762. Analytical RP-HPLC R_t = 20.2 min.

N-[(1*S*)-1-[(1*S*)-1-[(2-{2-[4-(2,6-Dioxo-1,3-dipropyl-2,3,6,9-tetrahydro-1*H*-purin-8-yl)phenoxy]acetamido}ethyl)carbamoyl]-2-hydroxyethyl]carbamoyl]-2-(4-hydroxyphenyl)ethyl]-(*E*)-6-((4-(2-(4,4-difluoro-5-(2-thienyl)-4-bora-3a,4a-diaza-*s*-indacene-3-yl)vinyl)phenoxy)acetamido)hexanamide **27**.



Compound **23** (5 μmol) was reacted with BODIPY 630/650-X-SE (2.8 μmol) according to General Procedure D. The residue was purified by preparative layer chromatography (15% MeOH/DCM) and then by semi-preparative RP-HPLC to give **27** (0.8 mg, 0.7 μmol , 25% from BODIPY 630/650-X-SE) as a blue solid. HRMS calculated for $\text{C}_{62}\text{H}_{69}\text{BF}_2\text{N}_{11}\text{O}_{11}\text{S}$ 1224.4960($\text{M}+\text{H}$)⁺; found 1224.4937. Analytical RP-HPLC R_t = 20.4 min.

N-[(1*S*)-1-[(1*S*)-1-[(2-{2-[4-(2,6-Dioxo-1,3-dipropyl-2,3,6,9-tetrahydro-1*H*-purin-8-yl)phenoxy]acetamido}ethyl)carbamoyl]-2-hydroxyethyl]carbamoyl]-2-(4-hydroxyphenyl)ethyl]-3-(4,4-difluoro-5,7-dimethyl-4-bora-3a,4a-diaza-*s*-indacene-3-yl)propanamide **28**.



Compound **23** (5 μmol) was reacted with BODIPY-FL-X-SE (2.6 μmol) according to General Procedure D. The residue was purified by silica plate (10% MeOH/DCM) and then by semi-preparative RP-HPLC to give **28** (0.7 mg, 0.7 μmol , 25% from BODIPY-FL-X-SE) as an orange solid. HRMS calculated for $\text{C}_{53}\text{H}_{67}\text{BF}_2\text{N}_{11}\text{O}_{10}$ 1066.5133($\text{M}+\text{H}$)⁺; found 1066.5176. Analytical RP-HPLC R_t = 18.0 min.

Pharmacology: General Methods

Cell lines and cell culture.

CHO cells expressing the A₁AR¹ (CHO-A₁) and CHO CRE-SPAP cells expressing the A₃AR² (CHO-A₃ SPAP) were used as previously described. Both cell lines were maintained in Dulbecco's modified Eagle's medium (DMEM) nutrient mix F12 (DMEM/F12) supplemented with 10% fetal calf serum and 2 mM L-glutamine at 37°C in a humidified atmosphere of air/CO₂.

Fluorescence-based competition binding assay.

This recently developed and fully characterised assay³ uses a fluorescent antagonist (in place of the more traditional radioligand) in combination with automated confocal imaging to allow affinity values of compounds to be determined at both the A₁AR and A₃AR.

CHO-A₃ SPAP or CHO-A₁ cells were seeded into the central 60 wells of a 96-well clear-bottomed, black-walled plate and grown to confluency. On the day of analysis, normal growth medium was removed and cells washed twice with HBSS pre-warmed to 37°C. Fresh HBSS was added to each well and the required concentration of unlabelled test compound was added. For experiments at the A₁AR and A₃AR using red-fluorescent tracer ligand **2**, the cells were incubated with the test compounds at 37°C for 30 min then 25 nM of **2** was added to each well and the cells incubated with the test compounds for a further 30 min at 37°C. For experiments at the using green-fluorescent tracer ligand **28**, the cells were incubated with the test compounds at 37°C for 2 h, then 25 nM of **28** was added to each well and the cells incubated for a further 30 min at 37°C. Buffer was then removed from each well, cells washed once in HBSS and fresh HBSS added at room temperature. Plates were immediately imaged using an ImageXpress Ultra confocal plate reader, which captured four central images per well using a Plan Fluor 40x NA0.6 extra-long working distance objective. **2** was excited at 635 nm and emission collected through a 640-685 nm band pass filter, and **28** was excited at 488 nm and emission collected through a 525-550 nm band pass filter. Total image intensity was obtained for each image collected using a multi-wave length cell scoring algorithm within the MetaXpress software (MetaXpress 2.0, Molecular Devices). This automated confocal imaging and analysis (refer to Data Analysis section in Supplementary Information) allowed determination of the amount of bound fluorescent ligand, and the resulting IC₅₀s obtained were used to calculate pK_i values for each of the compounds (Table 1, main paper).

[³H]-8-cyclopentyl-1,3-dipropylxanthine (DPCPX) whole cell competition binding assay.

CHO-A₁ cells were grown to confluence in white-sided, clear bottomed, 96 well plates. Media was removed from the cells and replaced with 100 μL serum-free media containing the required concentration of competing ligand, which was followed by the addition of 100 μL serum-free media containing [³H]DPCPX (0.40-1.1 nM). Non-specific binding was defined in the presence of 10 μM of **3**. Cells were incubated for 2 h at 37°C/5% CO₂. After 2 h, all media was removed from each well and cells washed twice with ice-cold phosphate-buffered saline. 100 μL Microscint 20 (PerkinElmer, Shelton, CT) was added per well, a white backing tape was added to the bottom and a sealant film to the top of each plate. The level of radioactivity per well was quantified using a TopCount scintillation counter (PerkinElmer).

CRE-SPAP gene transcription assay.

CHO-A₃ SPAP cells were grown to confluence in clear 96-well plates and serum starved for 18 h prior to experimentation in serum-free medium (DMEM/F12 supplemented with 2 mM L-glutamine). On the day of experiment, normal growth medium was removed and replaced with fresh serum-free medium and where appropriate three varying concentrations of test compound. Cells were incubated for 30 min at 37°C/5% CO₂, after which increasing concentrations of NECA were added and the cells incubated for a further 30 min, when 1 μM FSK was added to stimulate cAMP production within the cells. Cells were then incubated for 5 h, after which, all medium was removed and 40 μL of fresh serum-free medium added to each well, and cells incubated for a further 1 h at 37°C/5% CO₂. The plates were then incubated at 65°C for 30 min to destroy any endogenous alkaline phosphatases. Plates were cooled to room temperature, and 100 μL of 5 mM 4-nitrophenyl phosphate in diethanolamine-containing buffer [10% (v/v) diethanolamine, 280 mM NaCl, 500 μM MgCl₂, pH 9.85] was added to each well and incubated for 20 min at 37°C. The absorbance at 405 nm was measured using a Dynex MRX plate reader (Chelmsford, MA).

Data analysis.

All data were fitted using Prism 5 (GraphPad Software).

Competition binding curves with the fluorescently labelled antagonists, **2** and **28**, and [³H]DPCPX were fitted to the following equation to calculate the binding affinity (K_i) of the ligand to the receptor:

$$K_i = \frac{IC_{50}}{1 + \frac{[L]}{K_D}}$$

Where [L] is the concentration of **2**, **28** or [³H]DPCPX in nM and K_D is the K_D of **2**, **28** or [³H]DPCPX in nM. The calculated K_D values used were 17.0 nM and 3.11 nM for **2**, 316 nM and 11 nM, for **28** at A₁AR and A₃AR respectively, and 2.0 nM for [³H]DPCPX at A₁AR. The IC₅₀ is calculated from the following equation:

$$\% \text{ inhibition of specific binding} = \frac{100 \times [A]}{[A] + IC_{50}}$$

Where [A] is the concentration of competing drug and the IC₅₀ is the molar concentration of ligand required to inhibit 50% of the specific binding of concentration [L] of **2**, **28** or [³H]DPCPX.

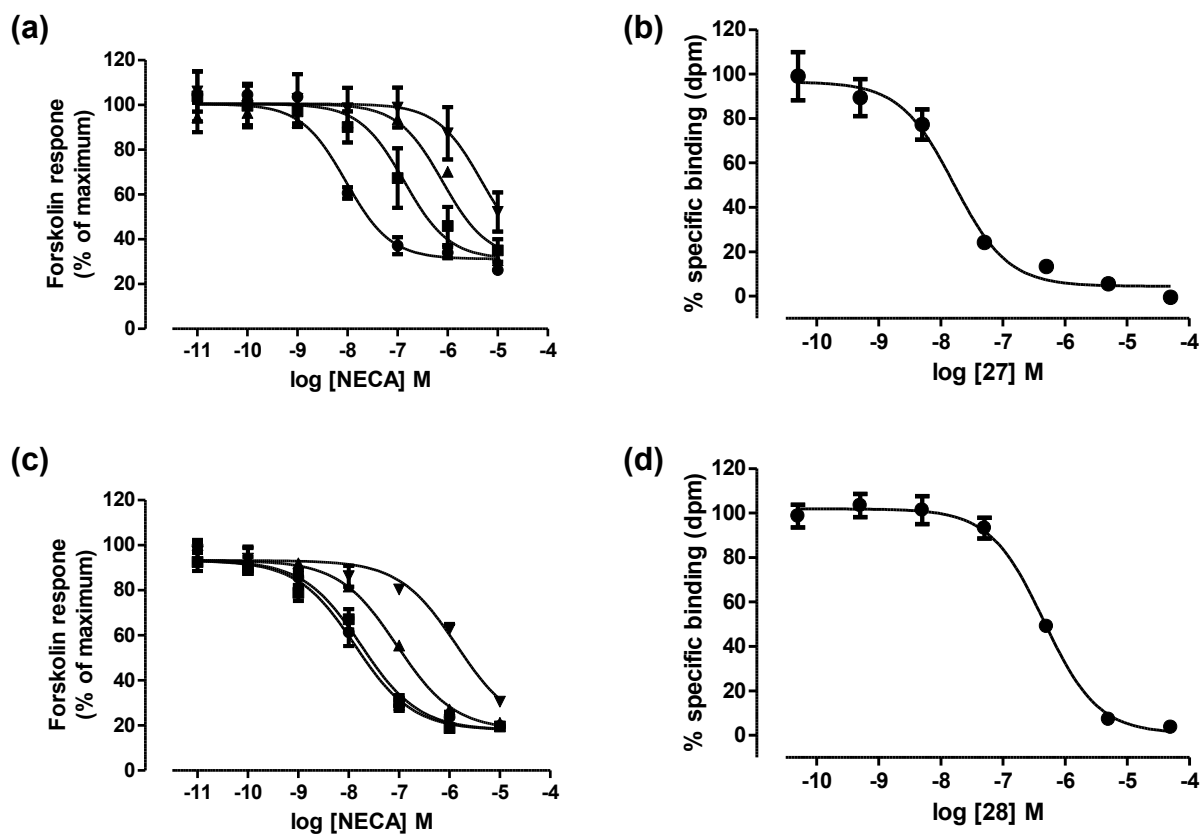
For the CRE-SPAP gene transcription assay, NECA concentration-response curves in the absence and presence of a range of concentrations of test compounds were globally fit to the following interaction model in Prism5.

$$\text{Response} = \frac{E_{\max} \times [A]}{([A] + EC_{50} \times \left(1 + \frac{[B]}{K_D}\right)^S)}$$

Where E_{max} is the maximal response, EC₅₀ is the molar concentration of NECA [A] in the absence of test compound required to generate a response that is 50% of E_{max}, [B] is the concentration of test compound, K_D is the antagonist equilibrium dissociation constant of the test compound and S is the Schild slope. For **1**, higher concentrations resulted in suppressed maxima of NECA concentration response curves. Estimated affinity values (pK_D) were therefore calculated from the shift of the agonist concentration response curves elicited in the presence of a single concentration of **1** (100 nM) which did not cause this effect using the following equation:

$$DR = 1 + \frac{[B]}{K_D}$$

Where DR (dose ratio) is the ratio of the agonist concentration required to stimulate an identical response in the presence and absence of a fixed concentration of antagonist, [B].



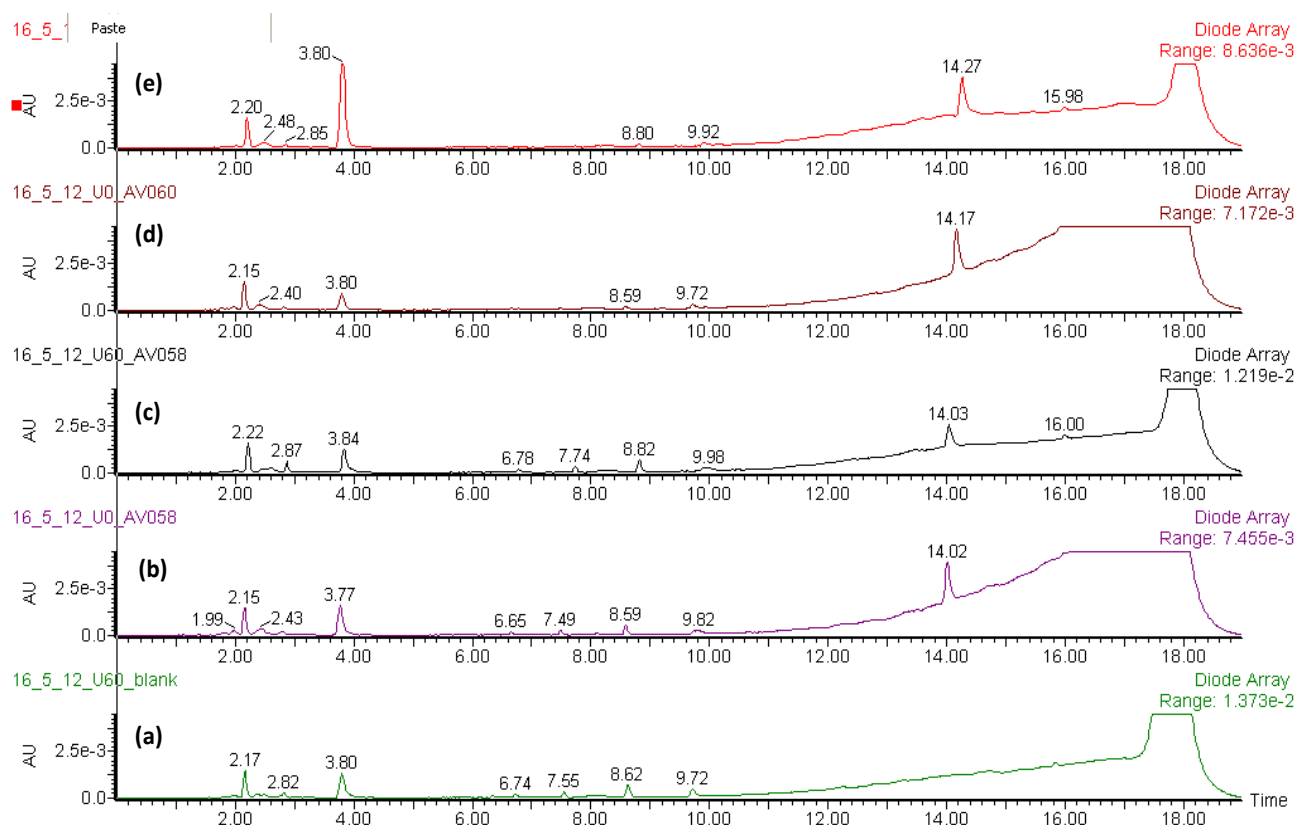
Supplementary Fig S1. Pharmacological analysis of **27** and **28** at A₃AR and A₁AR. (a and c) CHO-A₃ SPAP cells were stimulated with 1 μM FSK and increasing concentration of the agonist NECA (●). Parallel shifts in the NECA concentration response curve was observed in the presence of 10 nM (■), 100 nM (▲), and 1 μM (▼) (a) **27** or (c) **28**. Data are normalised to basal (in the absence of FSK) and 1 μM FSK SPAP production. Data represents the mean ± SEM from triplicate measurements. Data shown were obtained in a single experiment representative of four performed. . Inhibition of specific [³H]DPCPX binding by increasing concentrations of (b) **27** or (d) **28** in whole CHO-A₁ cells. Non-specific binding was determined in the presence of 10 μM of **3**. Each data point represents means ± SEM from triplicate measurements. Data shown were obtained in a single experiment representative of four performed.

	hA ₃ AR				hA ₁ AR			
	Fluorescent ligand-binding assay ^a		Functional SPAP assay ^c		Fluorescent ligand-binding assay ^b		Radioligand-binding assay ^d	
	pK _i	<i>n</i>	pK _B	<i>n</i>	pK _i	<i>n</i>	pK _i	<i>n</i>
3	7.80 ± 0.07	4	7.79 ± 0.32	4	7.30 ± 0.10	6	7.30 ± 0.07	4
8	8.95 ± 0.06	4	8.87 ± 0.15	4	7.49 ± 0.15	4	7.24 ± 0.06	3
13	8.49 ± 0.21	4	8.79 ± 0.19	6	7.66 ± 0.12	4	7.65 ± 0.12	4
19	7.26 ± 0.12	4	7.33 ± 0.15	5	7.04 ± 0.12	4	7.14 ± 0.08	4

Supplementary Table S2: Comparison of binding affinity of derivatised-XAC compounds using different assay formats. pK_i values were calculated from inhibition of the binding of fluorescent antagonist **2** to CHO-A₃ CRE-SPAP^a or CHO-A₁^b cells. ^c Measured by the shift in NECA-mediated inhibition of forskolin stimulated CRE-SPAP response in CHO CRE-SPAP cells expressing A₃AR. ^d Measured by inhibition of [³H]DPCPX binding in A₁AR expressing CHO cells. All values represent mean ± SEM for *n* separate experiments performed in duplicate (^{a-b}) or triplicate (^{c-d}).

Stability Analysis of Fmoc-dipeptide-XAC compounds under fluorescent assay conditions

The stability of compounds **5**, **6**, **8**, **9**, and **13**, as representative examples, were tested under the fluorescent binding assay conditions, in particular to confirm the stability of the carbamate moiety of the 9-fluorenylmethyloxycarbonyl group. The highest test concentration (0.01 mM) of the compound under assay conditions was determined as an appropriate level for RP-HPLC detection. The fluorescent ligand binding assay was performed as described in the Supplementary Information (see page S19), with a single 0.01 mM concentration of each test compound in duplicate, but with no addition of **2** after 30 mins. A 20 μL aliquot was taken immediately after test compound addition at t=0, and another 20 μL aliquot taken from the duplicate well after incubation at 37°C for 60 mins. A blank was also prepared containing no test compound, and aliquots taken at t=0 and 60 min time points. Aliquots removed from the assay were analysed immediately using analytical RP-HPLC, or stored in the freezer until the previous compound had been analysed. The RP-HPLC, analytical column, and solvent systems used for analysis were as described in the Experimental Section, but used a method of 0 - 1 min 10%B, 1 - 14 min gradient to 90%B, 14 - 15 min held at 90%B, 15 - 16 min gradient to 10%B, 16 - 19 min 10%B. The HPLC chromatograms of all compounds tested showed a peak corresponding to the test compound at both the t=0 and 60 min time point with no evidence of degradation products. Shown in Supplementary Fig S2 is a representative example, of **6** and **8**, and the blank measured at 60 min, see figure legend for details.



Supplementary Fig S2: Stability of test compounds under fluorescent binding assay conditions. (a) Blank at 60 mins. (b) **6** at 0 mins. (c) **6** at 60 mins. (d) **8** at 0 mins. (e) **8** at 60 mins. For (b) to (e) the test Fmoc-compound corresponds to the peak at approximately 14 minutes. (b) and (c) compound **6** is the peak at 14.0 min. (d) and (e) compound **8** is the peak at 14.2 min.

Fluorescent Confocal Microscopy Imaging studies.

Confocal microscopy was carried out essentially as described previously.² Briefly, cells were grown to approximately 80% confluency on 8-well Labtek chambered coverglasses (Nunc Nalgene) in DMEM/F12 supplemented with 10% FCS and 2mM L-glutamine. Cells were washed twice in HBSS, then incubated in the presence or absence of 100 nM MRS1220 for 30 min at 37°C. Cells were then incubated with compounds **1**, **24**, **27** or **28** for 30 min at room temperature, prior to collection of single equatorial confocal images. Concentrations used were equivalent to the K_D values determined in the functional assays (i.e., 0.5 nM **24**; 1 nM **27**; 10 nM **28**; and 30 nM **1**) to achieve equal receptor occupancies. Images were obtained on a Zeiss LSM510 Meta NLO confocal microscope using a 40x c-Apochromat 1.2NA water-immersion objective. For **1**, **24** and **27**, samples were excited using a 633nm HeNe laser, with emission collected through a BP650-710IR filter. For **28**, samples were excited using a 488nm Argon laser, and emission collected through an LP505 filter. In both cases a pinhole diameter of 1.5 Airy Unit was used and laser power, gain and offset kept the same for images taken in the presence and absence of MRS1220.

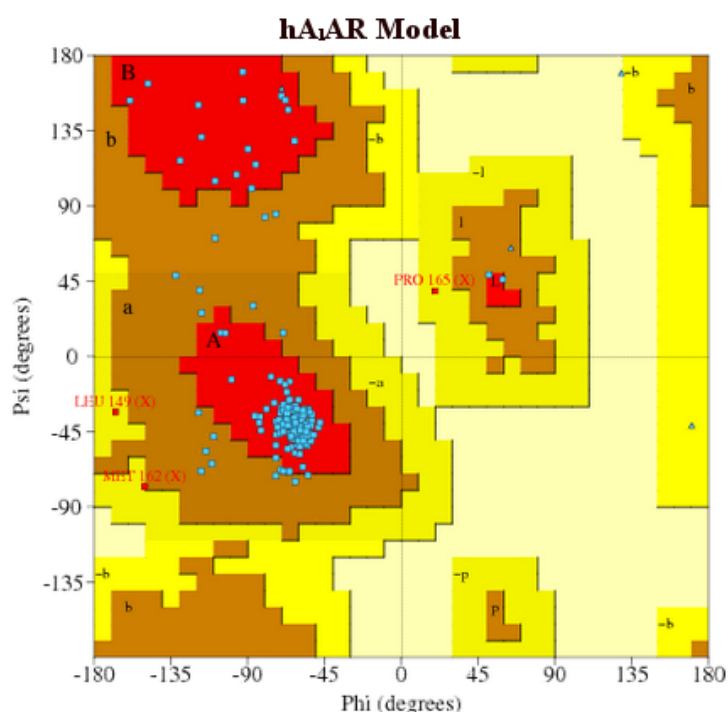
Molecular Modelling

The homology models of the A₁AR and A₃AR were constructed with SYBYL 6.5⁴ using the engineered adenosine A_{2A}AR crystal structure (3EML)⁵ as a template. The 160 residues long T4-lysozyme portion was deleted and the corresponding third intracellular loops (IL3) restored. The C- and N- termini were not built. The quality and integrity were checked with PROCHECK⁶ and WHATIF,⁷ and validation programs did not report any critical problems (see Supplementary Fig S3 and S4 for Ramachandran plots). After performing energy minimisation with the GROMOSG53a6 forcefield⁸ in GROMACS 4.5.3,⁹⁻¹¹ the models were inserted into a pre-equilibrated, fully solvated, POPC membrane bilayer. MD simulations were performed for 240 ns to generate a conformational ensemble with the co-crystallised ligand ZM241385 left in place throughout to maintain the general shape of the binding pocket. Water molecules were added utilising the single point charge (SPC)¹² model, 11 chloride ions were added as counterions, and a temperature of 310K was used whilst electrostatic interactions were treated with the smooth particle mesh Ewald (PME)¹³ method. Position restraints were initially applied to the heavy atoms of the A₁AR and A₃AR models along the x, y, and z axes as well as the phosphorus atom of POPC along the z axis only, where x-y is the membrane plane. The position restraints were gradually released during the timescale of the MD simulation.

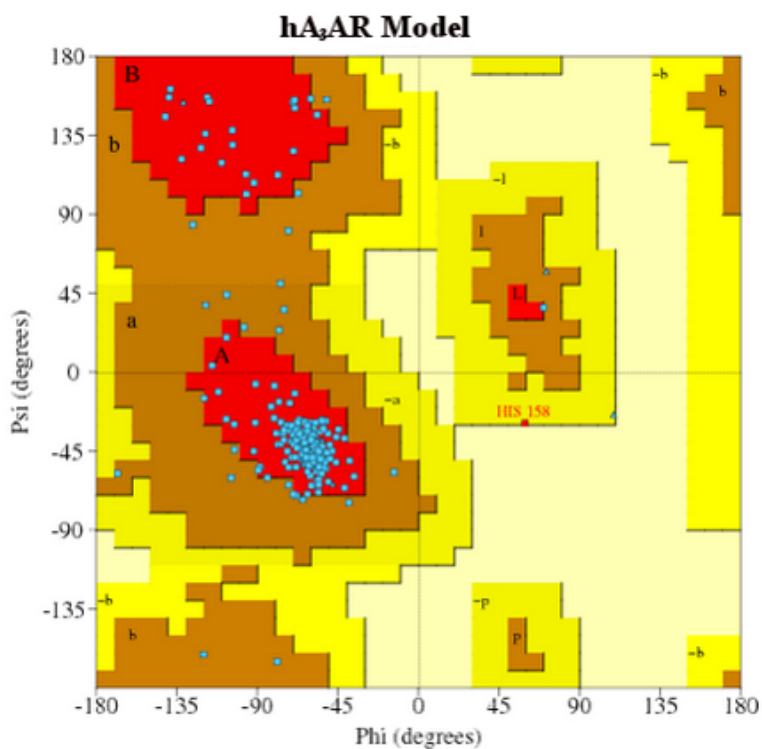
Protein models were chosen and extracted from the MD trajectory based on specific criteria, namely (1) the system was at as low an energy level as possible, (2) the critical and conserved Phe171 and Phe168 (in A₁AR and A₃AR respectively) which was found to interact with the xanthine rings in A_{2A}AR were making good pi-pi interactions with ZM241385. A selection of known antagonists were docked into these models for model validation using AutoDock 4.2.¹⁴ As Autodock reports a predicted K_i value for the ligands, this allows an easy and direct comparison with the corresponding experimental K_i values. The A₁AR and A₃AR models that gave the best R² value for experimental vs. predicted pK_i were selected (Supplementary Fig S5 and S6, Supplementary Tables S3 and S4).

Having validated the models, the docking program Glide¹⁵ was then used to dock **27** and **26** in the A₁AR and A₃AR models. The A₁AR and A₃AR models were overlaid with the 3-bound A_{2A}AR crystal structure (3REY) and **3** was used as the reference ligand to set a core reference position for the xanthine rings. The grid box sizes were set to 36 Å for the outer box and 14 Å for the inner to accommodate the relatively large ligands. The grid center was set by choosing the centroid of the reference ligand. The docking output parameters were as follow: the maximum number of poses to be written out per docking run was set to 100000, the number of poses that pass through the initial

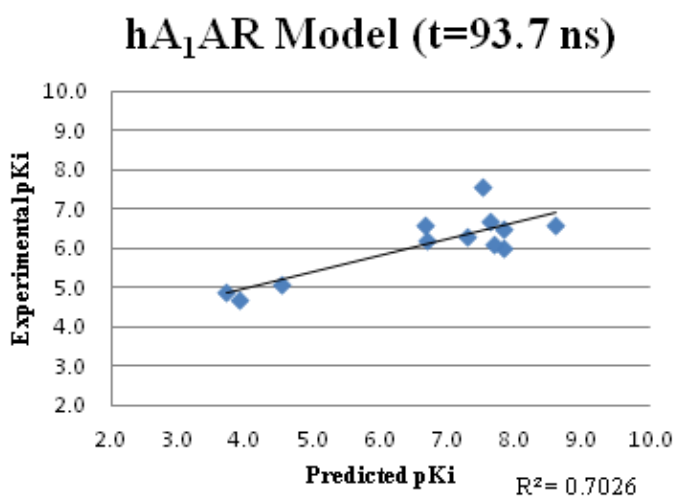
Glide screens was set to 50000, the number of poses kept for energy minimisation during docking was set to 1000, expanded sampling was used, the maximum number of energy minimisation steps was set to 10000, the sampling of amide was set to trans only, docking was restricted to 2.5 and 2.8 Å (adjustment required for generation of at least one docking output) from reference position for **27** and **26** respectively, the number of poses to be included for post-docking energy minimisation was set to 50, the maximum number of final poses to be written out was set to 50 per ligand, the cut off of Coulomb-vdW energy was set to 1.0 kcal/mol. Dockings were performed with standard precision (SP).¹⁶ Images were generated using Pymol and Chimera. Chimera¹⁷ is developed by the Resource for Biocomputing, Visualisation, and Informatics at the University of California, San Francisco, funded by grants from the National Institutes of Health National Center for Research Resources (2P41RR001081) and National Institute of General Medical Sciences (9P41GM103311).



Supplementary Fig S3. Ramachandran plot of hA₁AR model constructed using SYBYL 6.5. 89.6% of the residues were found in the most favored region; 9.3% were found in the additional allowed regions; 1.0% were found in the generously allowed regions and 0% were found in the disallowed regions.



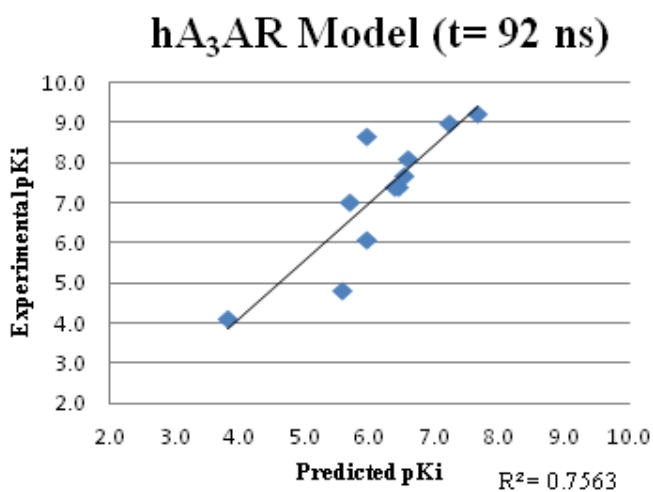
Supplementary Fig S4. Ramachandran plot of hA₃AR model constructed using SYBYL 6.5. 91.4% of the residues were found in the most favored region; 8.2% were found in the additional allowed regions; 0.4% were found in the generously allowed regions and 0% were found in the disallowed regions.



Supplementary Fig 5. Predicted pK_i vs. experimental pK_i for the series of known hA₁AR antagonists.

hA ₁ AR Antagonist	Predicted pK _i	Experimental pK _i
Caffeine	3.9	4.7 ¹⁸
Theophylline	3.7	4.9 ¹⁹
IBMX	4.5	5.1 ¹⁹
MRE3008 F20	7.8	6.0 ²⁰
AS99	7.7	6.1 ²⁰
L-97-1	6.7	6.2 ²¹
SCH58261	7.3	6.3 ²⁰
AS100	7.8	6.5 ²⁰
AS70	8.6	6.6 ²⁰
ZM241385	6.7	6.6 ²²
MRE2029 F20	7.6	6.7 ²⁰
XAC	7.5	7.6 ¹⁹

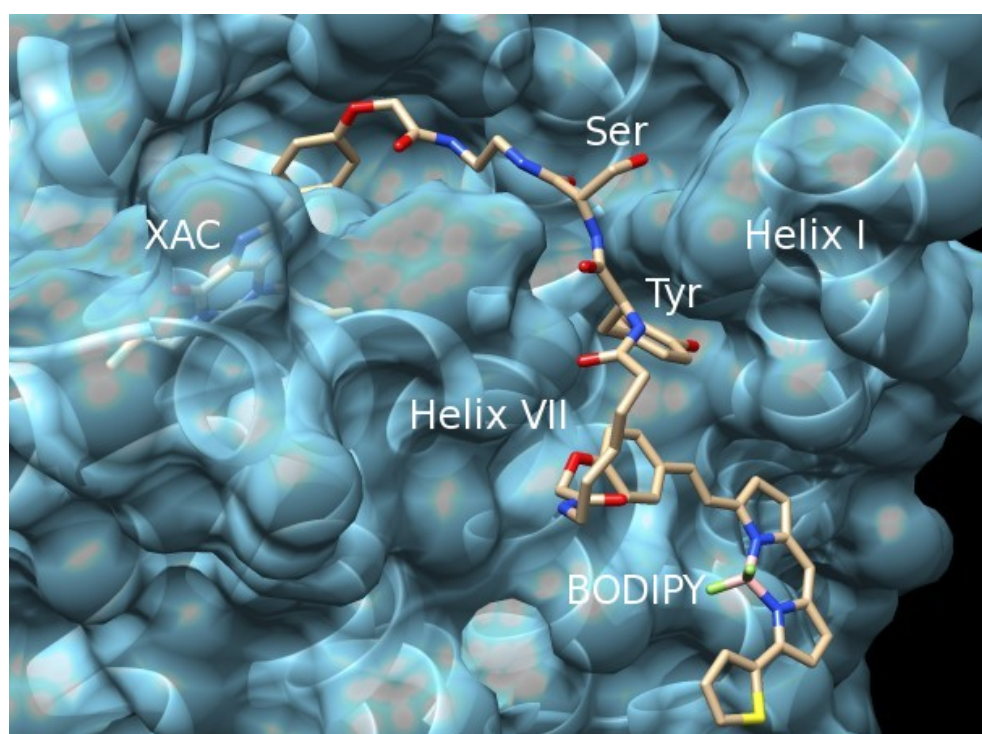
Supplementary Table S3. hA₁AR antagonists with AutoDock 4.2 predicted pK_i and the corresponding experimental pK_i.



Supplementary Fig S6. Predicted pK_i vs. experimental pK_i for the series of known hA₃AR antagonists.

hA ₃ AR Antagonist			Predicted pK _i	Experimental pK _i
Theophylline			3.8	4.1 ²³
Flavone			5.6	4.8 ²⁴
CGS15943			5.7	7.0 ²²
BWA1433			6.5	7.3 ²⁵
XAC			6.4	7.4 ²⁶
DPCPX			6.0	6.8 ²⁵
MRS1476			6.6	7.7 ^{27,28}
MRS1186			6.6	8.1 ²⁹
PSB11			5.9	8.7 ³⁰
MRE3008 F20	7.2	9.0 ²⁰		
MRS1220	7.7	9.2 ³¹		

Supplementary Table S4. hA₃AR antagonists with AutoDock 4.2 predicted pK_i and the corresponding experimental pK_i.



Supplementary Fig S7. Close-up view of the top-scoring pose of **27** bound to the A₃ receptor. The XAC, Ser, Tyr, and BODIPY moieties of the ligand are marked, and also the positions of helices I and VII. The semi-transparent molecular surface emphasises the way in which the XAC portion of the ligand accesses the adenosine binding site while the dipeptide linker lies in the cleft between helices I and VII, permitting the fluorophore to tuck into the interface between the protein and the lipid bilayer (not shown).

References

1. Y. Cordeaux, S. J. Briddon, A. E. Megson, J. McDonnell, J. M. Dickenson, S. J. Hill, *Mol. Pharmacol.*, 2000, **58**, 1075–1084.
2. A. J. Vernall, L. A. Stoddart, S. J. Briddon, S. J. Hill, B. Kellam, *J. Med. Chem.*, 2012, **55**, 1771–1782.
3. L. A. Stoddart, A. J. Vernall, J. L. Denman, S. J. Briddon, B. Kellam, S. J. Hill, *Chem. Biol.*, 2012, **19**, 1105–1115.
4. SYBYL Biopolymer modelling manual, version 6.5, Tripos Inc., 1998.
<http://www.tripos/cpm>.
5. V.-P. Jaakola, M. T. Griffith, M. A. Hanson, V. Cherezov, E. Y. T. Chien, J. R. Lane, A. P. Ijzerman, R. C. Stevens, *Science*, **2008**, 322, 1211–1217.
6. R. A. Laskowski, M. W. MacArthur, D. S. Moos, J. M. Thornton, *J. Appl. Cryst.*, 1993, **26**, 283–291.
7. G. Vriend, *J. Mol. Graph.*, 1990, **8**, 52-56.
8. C. Oostenbrink, A. Villa, A. E. Mark, W. F. van Gunsteren, *J. Comput. Chem.*, 2004, **25**, 1656–1676.
9. H. J. C. Berendsen, D. van der Spoel, and R. van Drunen, *Comput. Phys. Commun.*, 1995, **91**, 43–56.
10. D. Van Der Spoel, E. Lindahl, B. Hess, G. Groenhof, A. E. Mark, H. J. C. Berendsen, *J. Comput. Chem.*, 2005, **26**, 1701–1718.
11. B. Hess, C. Kutzner, D. Van Der Spoel, E. Lindahl, *J. Chem. Theory Comput.*, 2008, **4**, 435-447.
12. H. J. C. Berendsen, W. F. van Gunsteren, and J. Hermans, in *In Intermolecular Forces*, ed. B. Pullman, Reidel Publishing Company, 1981, p. 331.
13. U. Essmann, L. Perera, M. L. Berkowitz, T. Darden, H. Lee, L. G. Pedersen, *J. Chem. Phys.*, 1995, **103**, 8577-8593.
14. G. M. Morris, R. Huey, W. Lindstrom, M. F. Sanner, R. K. Belew, D. S. Goodsell, A. J. Olson, *J. Comput. Chem.*, 2009, **30**, 2785–2791.
15. *Glide, version 5.8*, Schrödinger, LLC, New York, N.Y., 2012.
16. R. A. Friesner, J. L. Banks, R. B. Murphy, T. A. Halgren, J. J. Klicic, D. T. Mainz, M. P. Repasky, E. H. Knoll, M. Shelley, J. K. Perry, D. E. Shaw, P. Francis, P. S. Shenkin, *J. Med. Chem.*, 2004, **47**, 1739–1749.
17. E. F. Pettersen, T. D. Goddard, C. C. Huang, G. S. Couch, D. M. Greenblatt, E. C. Meng, T. E. Ferrin, *J. Comput. Chem.*, 2004, **25**, 1605–1612.

18. J. Deckert, W. Berger, K. Kleopa, S. Heckers, G. Ransmayr, H. Heinsen, H. Beckmann, and P. Riederer, *Neuroscience Letters*, 1993, **150**, 191–194.
19. R. Jockers, M. E. Linder, M. Hohenegger, C. Nanoff, B. Bertin, A. D. Strosberg, S. Marullo, M. Freissmuth, *J. Biol. Chem.*, 1994, **269**, 32077–32084.
20. K. Varani, S. Gessi, S. Merighi, F. Vincenzi, E. Cattabriga, A. Benine, K. N. Klotz, P. G. Baraldi, M. A. Tabrizi, S. M. Lennan, E. Leung, P. A. Borea, *Biochem Pharmacol.*, 2005, **70**, 1601-1612.
21. P. C. M. Obiefuna, V. K. Batra, A. Nadeem, P. Borron, C. N. Wilson, S. J. Mustafa, *J. Pharmacol. Exp. Ther.*, 2005, **315**, 329–336.
22. E. Ongini, S. Dionisotti, S. Gessi, E. Irenius, B. B. Fredholm, *Naunyn Schmiedebergs Arch. Pharmacol.*, 1999, **359**, 7–10.
23. K. N. Klotz, J. Hessling, J. Hegler, C. Owman, B. Kull, B. B. Fredholm, M. J. Lohse, *Naunyn Schmiedebergs Arch. Pharmacol.*, 1998, **357**, 1–9.
24. Y. Karton, J. L. Jiang, X. D. Ji, N. Melman, M. E. Olah, G. L. Stiles, K. A. Jacobson, *J. Med. Chem.*, 1996, **39**, 2293–2301.
25. C. A. Salvatore, M. A. Jacobson, H. E. Taylor, J. Linden, R. G. Johnson, *Proc. Natl. Acad. Sci. U.S.A.*, 1993, **90**, 10365–10369.
26. K. Varani, S. Merighi, S. Gessi, K. N. Klotz, E. Leung, P. G. Baraldi, B. Cacciari, R. Romagnoli, G. Spalluto, P. A. Borea, *Mol. Pharmacol.*, 2000, **57**, 968–975.
27. A.-H. Li, S. Moro, N. Melman, X.-D. Ji, K. A. Jacobson, *J. Med. Chem.*, 1998, **41**, 3186–3201.
28. D. L. Kirlpatrick, S. Watson, S. Ulhaq, in *Structure-based drug design: Combinatorial chemistry and molecular modeling*, Bentham Science Publishers BV: Boca Raton, 1999, **Vol 2**.
29. Y. C. Kim, X. D. Ji, K. A. Jacobson, *J. Med. Chem.*, 1996, **39**, 4142–4148.
30. C. E. Müller, M. Diekmann, M. Thorand, V. Ozola, *Bioorg. Med. Chem. Lett.*, 2002, **12**, 501–503.
31. K. A. Jacobson, K.-S. Park, J.-L. Jiang, Y.-C. Kim, M. E. Olah, G. L. Stiles, X.-D. Ji, *Neuropharmacology*, 1997, **36**, 1157–1165.

NMR spectra and HPLC chromatograms

